

Vladimír Vanýsek; Jan Svatoš
Solid particles in reflection nebulae. I.

Acta Universitatis Carolinae. Mathematica et Physica, Vol. 5 (1964), No. 1, 1--[18a]

Persistent URL: <http://dml.cz/dmlcz/142160>

Terms of use:

© Univerzita Karlova v Praze, 1964

Institute of Mathematics of the Academy of Sciences of the Czech Republic provides access to digitized documents strictly for personal use. Each copy of any part of this document must contain these *Terms of use*.



This paper has been digitized, optimized for electronic delivery and stamped with digital signature within the project *DML-CZ: The Czech Digital Mathematics Library* <http://project.dml.cz>

SOLID PARTICLES IN REFLECTION NEBULAE. I.

PEVNÉ ČÁSTICE V REFLEXNÍCH MLHOVINÁCH. I.

ТВЕРДЫЕ ЧАСТИЦЫ В ОТРАЖАТЕЛЬНЫХ ТУМАННОСТЯХ. I

VLADIMÍR VANÝSEK and JAN SVATOŠ

Astronomical Institute of the Charles University, Prague

Director Prof. Dr. J. M. Mohr

(Received September, 30, 1963)

1. INTRODUCTION

A study of interstellar solid particles is very important at present from the point of view of the evolution of these very small solid particles in cosmic space. Apart from selective interstellar absorption and polarization it is possible to study their physical nature only in reflection nebulae. A choice of suitable objects for such work is very difficult due to the fact that only small objects of a similar kind have a pronounced continuous spectrum. Shain, Gaze and Pikelner [1] give in their catalogue a number of cases with combined emission spectrum and continuum but only quite a small number with continuous spectrum which would simultaneously have sufficient surface luminous intensity. Among the most suitable cases is NGC 7023, which has already been studied by a number of authors and which a more detailed experimental analysis shows to be indisputably suitable. The first such study was made photographically by Keenan [2] in 1936 but the influence of the background was not sufficiently eliminated by reduction. In a later study Collins [3] repeated the measurement and again explained the difference in colour of the illuminating star and nebula. Later these measurements were discussed by Henyey and Greenstein [4] in 1938. All these measurements were performed using the photographic method and were naturally hampered by the errors corresponding to this method. Between 1955 and 1960 several photoelectric measurements were made by Martel [5] and M. H. Johnson [6]. The polarization photographic measurements, which deserve mention, can be found in the paper by Martel and the photoelectric measurements in the paper by Johnson. The dependence of the polarization on the wave-length of light can be found in a short communication by Gehlers [7]. Grygar [8] dealt in greater detail recently with the photographic photometry of this nebula. All these measurements show the clear blue colour excess of the nebula compared with the illuminating star. An exception are the findings of Keenan who arrived at distinctly positive excesses.

2. BASIC DATA OF NGC 7023

The reflection nebula NGC 7023 ($21^{\text{h}}01^{\text{m}}, +67^{\circ}58'$ equin. 1950) has an apparent dimension in blue light in the Mt. Palomar atlas of about $19'$. It is illuminated by the star HD 200 775 of spectral type $B_3\text{ne V}$. According to Mendoza [9] it is distinguished by a pronounced emission in H_{α} and H_{β} with clear shell characteristics. The last measurement was coupled in the international UBV system to the photometric standard HD 219 314 and to check the colour system the star BD + 55°215 of the type $B_1\text{II}$, with $B - V = +0.15$, $U - B = -0.69$, was used during measurement. The polarization of this star was measured by Hall [10]. It is not larger than 1% (0.007). The intrinsic colour of the star, derived from the spectral type neglecting, of course, the occurrence of emission, would be according to H. L. Johnson [11]

$$B - V = -0.20, \quad U - B = -0.71.$$

Thus the absorption would be

$$B - V = 0.60, \quad U - B = 0.31.$$

The region around this nebula is distinguished by absorbing clouds symmetrically distributed about the nebula, and clearly seen on reproductions of the Palomar atlas. In this region E. B. Watson [12] and also Rosino and Romano [13] found a larger quantity of irregular variables, mostly of the type T Tauri, which obviously have a geometrical connection.

Table I. Photometrical data for HD 200 775

| Author | P _v | V | C _e | B-V | U-B |
|---------|----------------|------|----------------|-------|-------|
| Martel | 7.27 | — | +0.30 | — | — |
| Johnson | — | 7.32 | — | +0.45 | -0.48 |
| 1962 | — | — | — | +0.41 | — |
| Vanýsek | — | 7.30 | — | +0.40 | -0.43 |
| 1963 | — | — | — | — | — |

The surface brightness in the maximally bright region of the nebula is approximately $v = 20^{\text{m}}$ for a square arc second. Table II gives a brief survey of the surface brightnesses measured by different authors. The large differences are understandable in view of the irregular brightness distribution and thus the irregular shape of the nebula itself.

Table II. Surface brightness for a square second of arc

| Author | □ "m | Remarks |
|---------|-------|-------------------------|
| Keenan | 21.7 | mean value |
| Collins | 21.78 | photographic mean value |
| Grygar | 22.9 | 1.1'S |
| | 22.79 | 1.6'E |
| Martel | 20.58 | 0.8'S |
| Johnson | 23.2 | photoelectric 3' N |
| | 22.91 | 1.5'NE |
| Vanýsek | 20.77 | 1.0'N |

The structure of the nebula is *best* seen on detailed isophotometric maps obtained photometrically by Grygar [8]. In agreement with him Martel [5] finds a pronounced elongation of the nebula in a position angle of 190° which is very probably caused by the irregular structure of the dark mass before the nebula.

3. DEFINITION AND DETERMINATION OF COLOUR DIFFERENCE E OF NEBULA

The colour difference which is to be determined is defined by

$$(1) \quad E = (B - V)_{st} - (B - V)_{neb}$$

where $(B - V)_{st}$ is the colour index of the star and $(B - V)_{neb}$ of the nebula in the international system. If it holds for conversion from the instrumental to the international system that

$$(2) \quad B - V = A_1 + A_2 [b - v]$$

then for the difference it is enough to know the value of the coefficient A_2 , since

$$(3) \quad E = A_2 [(b - v)_{st} - (b - v)_{neb}]$$

which according to experience is suitable, while the coefficient A_1 , which is subject to considerable variations, need not be determined separately. The elimination of the colour coefficient of extinction can be carried out by direct measurement of some near stars of different spectral types so that it is included in the value of A_2 .

The actual photoelectric measurements in a nebula were made in two ways: on the one hand by measuring in previously fixed points of the nebula, and on the other hand by photometric cuts in the direction of daily motion. The apparent daily motion of the object over the diaphragm of the photometer was used for the photometric cuts since the nebula has high declination. The series from 28. 8. 1962 was chosen from several series of measurements for treatment by photometric cuts with a diaphragm $103''$ in diameter in B and V and a second series, from 14. 9. 1963, for measurement in a stable diaphragm of $103''$ and through the point of connection of the stellar brightness to the standard. In neither case did the value of the air mass during the measurements exceed $z = 1.25$. The internal accuracy fluctuated between 5 % and 1 %.

Measurement was performed with a 65 cm reflector with photoelectric photometer, designed by P. Mayer [14], in the BV system in 1962 and in 1963 in the UVV system, supplemented by an abbreviated range at the region denoted here by C with effective wave-length around 3800 Å.

Those regions on the photometric cuts where the intensity did not fall below the limit guaranteeing a higher accuracy than 5 % were chosen. The traces of the nebula in the record itself were detectable at approximately double the length of the used cut. Measurement was made in the cut above the star and in two directions. One was north and the other south of the star, as can be seen from the cut indicated in the reproduction of a Palomar chart. The results of measurement are given in Tabs. III and IV.

Table III

| Tracing: | across the star | | 70''S of the star | | 70''N of the star |
|----------|-----------------|-------|----------------------|-------|----------------------|
| | r | E | r | E | E |
| West | 0.39 | -0.14 | 0.33 | +0.22 | +0.16 |
| | 0.37 | -0.23 | 0.31 | +0.14 | +0.27 |
| | 0.35 | -0.22 | 0.29 | -0.08 | +0.30 |
| | 0.33 | -0.17 | 0.27 | -0.14 | +0.08 |
| | 0.31 | -0.08 | 0.26 | -0.22 | -0.08 |
| | 0.29 | -0.08 | 0.25 | -0.16 | -0.15 |
| | 0.27 | -0.30 | 0.23 | -0.14 | -0.10 |
| | 0.25 | -0.43 | 0.22 | -0.19 | -0.14 |
| | 0.23 | -0.48 | 0.21 | -0.22 | -0.17 |
| | 0.21 | -0.48 | 0.20 | -0.18 | -0.17 |
| | 0.20 | -0.52 | 0.19 | -0.18 | -0.21 |
| | 0.18 | -0.54 | 0.18 | -0.23 | -0.31 |
| | 0.16 | -0.46 | 0.18 | -0.20 | -0.23 |
| | 0.14 | -0.35 | 0.18 | -0.18 | -0.09 |
| | 0.12 | -0.41 | 0.18 | -0.18 | -0.05 |
| | East | 0.10 | -0.07 | 0.18 | -0.18 |
| 0.12 | | -0.17 | 0.18 | -0.14 | +0.08 |
| 0.14 | | -0.42 | 0.18 | -0.26 | +0.01 |
| 0.16 | | -0.44 | 0.18 | -0.32 | +0.02 |
| 0.18 | | -0.57 | 0.19 | -0.30 | -0.03 |
| 0.20 | | -0.33 | 0.20 | -0.35 | -0.02 |
| 0.21 | | -0.34 | 0.21 | -0.47 | 0.00 |
| 0.23 | | -0.30 | 0.22 | -0.51 | +0.03 |
| 0.25 | | -0.33 | 0.23 | -0.55 | +0.05 |
| 0.27 | | -0.32 | 0.25 | -0.52 | +0.11 |
| 0.29 | | -0.28 | 0.26 | -0.35 | +0.11 |
| 0.31 | | -0.22 | 0.27 | -0.35 | +0.11 |
| 0.33 | | -0.17 | 0.29 | -0.34 | +0.16 |
| 0.35 | | -0.25 | 0.31 | -0.16 | +0.09 |
| 0.37 | | -0.30 | 0.33 | -0.01 | +0.19 |
| 0.39 | | -0.14 | 0.35 | -0.06 | +0.23 |

r — distance from the star; $1r = 12'$.

Table IV. Measurements with 103'' diaphragm centred at 70'' south of the star

| | B-V | U-B | U-C |
|-----------|----------------|----------------|-------|
| E star | -0.25 -0.40 | -0.25 -0.40 | -0.08 |

The values of r in Tab. III are the distances from the central star calculated in units of $r = 1 = 12'$, where $12'$ is the effective radius of the nebula, which will be dealt with later.

Tables V and VI compare the values found by Martel, who determined the nebula by a diaphragm also marking $34''$ on the object measured.

Table V. Distribution of E in the nebula according to Martel

| | W | | | E | |
|-------|-------|-------|-------|-------|-------|
| | 1'6 | 0'8 | 0'0 | 0'8 | 1'6 |
| N 0'8 | | | -0.01 | | |
| 0'0 | -0.34 | -0.07 | | -0.41 | -0.34 |
| S 0'8 | | | -0.28 | | |

Table VI. Distribution of E in the nebula according to our measurements

| | | W | | | | E | | | | |
|---|-----|-------|-------|-------|-------|-------|-------|-------|-------|-------|
| | | 4' | 3' | 2' | 1' | 0'0 | 1' | 2' | 3' | 4' |
| N | 1'2 | — | +0.27 | -0.13 | -0.21 | -0.02 | -0.03 | +0.05 | +0.16 | — |
| | 0'0 | -0.20 | -0.40 | -0.50 | -0.41 | | -0.08 | -0.44 | -0.33 | -0.20 |
| S | 1'2 | — | +0.14 | -0.15 | -0.18 | -0.18 | -0.32 | -0.50 | -0.10 | — |

4. COMPARISON OF RESULTS OF OBSERVATIONS WITH OTHER AUTHORS

Our values in Tab. VII are derived from photometric cuts so that it was possible to eliminate the influence of a weak star, which in Martel's measurements is seen as a decrease in the value of E from 0.8'E to -0.07 . Our value of E , found south of the star -0.23 , is obtained from the average of a large number of measurements in 1962. The measurement in 1963 (Tab. IV) with a much larger diaphragm differs only in the limits of errors.

The earlier measurements of 1936 showed that reflection nebulae are all more blue than the illuminating star itself. A number of authors substantially confirmed this fact. The following table (VIII) gives a survey of all the more important measurements mentioned. On the whole, it is seen that the colour difference between the star and the nebula is on an average $E = -0.25$ in the UBV system. It is also seen that the maximum value of the negative excess is SE of the central star practically in the projection of the isophotos in the direction of a position angle of $190^\circ \div 200^\circ$, and thus even in places where Martel found maximum polarization. If we compare the total colour excess of NGC 7023 with the colour excesses of other nebulae of the reflection type, we see that it does not differ very much. For example, Johnson [6] gives for 10 different objects $\bar{E} = -0.20$ in the BV system.

On the other hand, it should be noted that the northern part of the nebula has a low colour excess, on an average around 0, which also follows from the measurements of Martel and Keenan. In the direction $40''$ NW of the central star Keenan found places with positive excess, i. e. a region where the nebula should be redder than the star itself. Although we admit a large error in the photographic measurements of Keenan, it is certain that the high excess in his measurement ($+0.55$) is already outside the limits of measuring errors. We are therefore justified in thinking that our measurements, which in these area show circa $+0.20$, are the real value of the colour excess. Martel did not measure in these places.

Our results agree to a certain extent with those of Khatchikian [15], published in a paper by Parsamian [16].

5. EMISSION IN NEBULA

According to Greenstein and Aller [17] a nebula exhibits emission in H_α and H_β . The measurements by Johnson [6] with interference filters also show an excess of light in the neighbourhood of H_β . However, Greenstein himself points out that this is the reflection of the emission lines of the star itself in the nebula. Unfortunately, good enough spectrophotometric data, which might definitely decide this question, are not available. Shain, Gaze and Pikelner call this nebula a mixed nebula, but this can be explained by the reflection of the pronounced emission lines H_α and H_β . If the results obtained by Grygar are also judged from this point of view, it is seen that the decrease in brightness in the region of H_α of this nebula was very sudden and the isophotometric measurements show rather that, at the most in the immediate neighbourhood of the star itself, can we calculate with a certain unsubstantial emission in H_α . We are therefore justified in thinking that as long as there exists an emission component in the nebula itself, then it has a completely insignificant share in the total intensity of the continuous spectrum. Martel in her paper adds that she found no emission line for this nebula. We can thus regard this object as an object shining only by the scattered light of the central star.

6. INTRINSIC ABSORPTION IN NEBULA

According to the intrinsic colour of the star and the measured colour excess CE we arrive, on the basis of the relation

$$(4) \quad A = \gamma \times CE$$

a total absorption A of 1.8, if a value of $\gamma = 3$ is assumed.

The share of the intrinsic absorption in a nebula can only be estimated. Nevertheless, according to the extent of the absorbing mass around the central star, about 80 % of the total absorption can be ascribed to the immediate surroundings, i. e. to the nebula itself. According to this the absorption in the nebula is about 1.5. Of course, it is lower than would appear from the earlier measurements of Stebbins, Huffer and Whitford [18] from 1940, where the total absorption was 2.1. The optical depth of the whole absorbing material will be approximately 1.4. If it is assumed below that the actual region of shining nebula is about 0.6 of the total region of dark mass, we arrive at an optical depth very near to 1.

7. INTERPRETATION OF MEASUREMENTS

The measurements, the results of which are given in the preceding paragraphs, can be interpreted by comparing them with theoretical models. In 1938 Henyey and Greenstein [4], somewhat later Schalén [19] and quite recently Van Houten [20] dealt with an analogous problem. In all of these cases, however, the actual interpretation of the theory assumed absorbing particles with relatively low albedo. Nevertheless, it is clear that the albedo

of interstellar dust is high and that therefore these were either dielectric particles without absorption inside the body itself or particles with a conducting nucleus, e. g. carbon, covered with a layer of ice, as was shown not long ago by Hoyle and Wickramasinghe [21] and Wickramasinghe [22]. For the time being, therefore, we shall deal mainly with dielectric particles with refractive index near to that of water ($m = 1.33$) or silicates.

A very important factor in our considerations is the geometry of the nebular formation, which plays a significant role. We studied altogether four models which, although simplified from the geometrical aspect, represent reality at least approximately. In all the models, which are axially symmetrical, the star is placed in the centre of symmetry. The models are:

1. spherical cloud
2. cloud in form of annular sphere.
3. cloud in form of spherical layer where illuminating star is further in direction of line of sight than nebula
4. cloud in form of spherical layer where illuminating star is nearer than nebula in direction of line of sight.

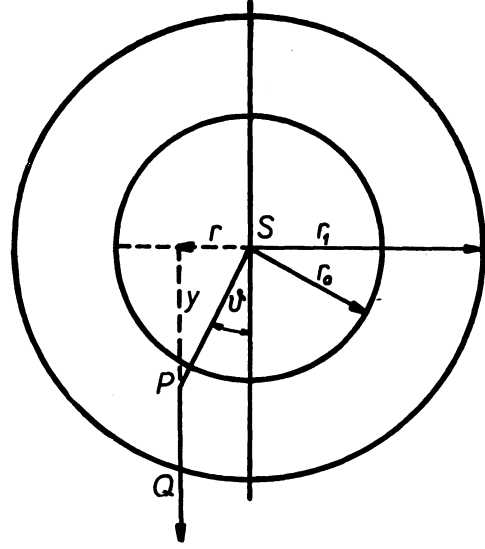


Fig. 1.

We shall now derive in detail the relations required for model 2, which

is the most general and the other models are defacto composed of this model from the mathematical point of view. Therefore, let a dark mass of homogeneous density be distributed around an illuminating star in the form of an annular sphere (Fig. 1). Let us take an element in the direction of observation and of unit cross-section and length dy , containing the point P. The scattered light in this element, contributing to the scattered light in the direction \overline{PQ} , is given by the expression

$$(5) \quad dI(r) = I_s \omega dy e^{-k(\overline{SP} - r_1 + \overline{PQ})} S(\vartheta)$$

where I_s is the energy irradiated by the star into a unit solid angle, ω is the solid angle under which the element is seen from the point S. k = coefficient of absorption.

$S(\vartheta)$ is the so-called scattering function which will be dealt with later. It is clear from Fig. 1 that

$$(6) \quad \overline{SP} = r \operatorname{cosec} \vartheta; \quad \overline{PQ} = \sqrt{r_1^2 - r^2} - r \cotg \vartheta;$$

$$\omega = (r^2 \operatorname{cosec}^2 \vartheta)^{-1}.$$

Further:

$$y = r \cotg \vartheta; \quad dy = r \operatorname{cosec}^2 \vartheta d\vartheta$$

Substituting these relations in (5) gives

$$(7) \quad dI(r) = I_s r^{-1} \exp. [-k\sqrt{r_1^2 - r^2} - r_0] \exp. [-kr (\operatorname{cosec} \vartheta - \cotg \vartheta)] \mathbf{S}(\vartheta) d\vartheta$$

The total brightness of the nebula at a distance r from the centre of the nebula S is given by integration

$$(8a) \quad \left\{ \begin{aligned} I(r) = I_s r^{-1} \exp. [-k(\sqrt{r_1^2 - r^2} - r_0)] & \left\{ \int_{\arcsin \frac{r}{r_1}}^{\arcsin \frac{r}{r_0}} \exp. [-kr (\operatorname{cosec} \vartheta - \cotg \vartheta)] \mathbf{S}(\vartheta) d\vartheta + \right. \\ & \left. + \int_{\pi - \arcsin \frac{r}{r_0}}^{\pi - \arcsin \frac{r}{r_1}} \exp. [-kr (\operatorname{cosec} \vartheta - \cotg \vartheta)] \mathbf{S}(\vartheta) d\vartheta \right\} \end{aligned} \right.$$

if $r < r_0$, and

$$(8b) \quad I(r) = I_s r^{-1} \exp. [-k(\sqrt{r_1^2 - r^2} - r_0)] \int_{\arcsin \frac{r}{r_1}}^{\pi - \arcsin \frac{r}{r_1}} \exp. [-kr (\operatorname{cosec} \vartheta - \cotg \vartheta)] \mathbf{S}(\vartheta) d\vartheta$$

if $r \geq r_0$;

It is easily seen that (8b) is actually the formula for model 1, if $r_0 = 0$, for a spherical nebula. Analogical relations hold for models 3 and 4. For model 3:

$$(9a) \quad I(r) = I_s r^{-1} \exp. [-k(\sqrt{r_1^2 - r^2} - r_0)] \int_{\arcsin \frac{r}{r_1}}^{\arcsin \frac{r}{r_0}} \exp. [-kr (\operatorname{cosec} \vartheta - \cotg \vartheta)] \mathbf{S}(\vartheta) d\vartheta$$

if $r < r_0$

$$(9b) \quad I(r) = I_s r^{-1} \exp. [-k(\sqrt{r_1^2 - r^2} - r_0)] \int_{\arcsin \frac{r}{r_1}}^{\frac{1}{2} \pi} \exp. [-kr (\operatorname{cosec} \vartheta - \cotg \vartheta)] \mathbf{S}(\vartheta) d\vartheta$$

if $r \geq r_0$

For model 4:

$$(10a) \quad I(r) = I_s r^{-1} \exp. [-k(\sqrt{r_1^2 - r^2} - r_0)] \int_{\pi - \arcsin \frac{r}{r_0}}^{\pi - \arcsin \frac{r}{r_1}} \exp. [-kr (\operatorname{cosec} \vartheta - \cotg \vartheta)] \mathbf{S}(\vartheta) d\vartheta$$

if $r < r_0$

$$(10b) \quad I(r) = I_s r^{-1} \exp. [-k(\sqrt{r_1^2 - r^2} - r_0^2)] \int_{\frac{1}{2} \pi}^{\pi - \arcsin \frac{r}{r_1}} \exp. [-kr (\operatorname{cosec} \vartheta - \cotg \vartheta)] \mathbf{S}(\vartheta) d\vartheta$$

if $r \geq r_0$

Since the absolute values I_s will not be needed in calculating the intrinsic ratios of the intensities in the two wave-length regions, let us put $I_s = 1$; $k = 1$.

8. DEFINITIONS OF $\mathbf{S}(\vartheta)$

The definition of the scattering function is derived from Mie's theory. Starting from the Maxwell equations

$$(11) \quad \text{rot } \mathbf{H} = ikm^2 \mathbf{E}$$

$$\text{rot } \mathbf{E} = -ik\mathbf{H}$$

where \mathbf{E} , \mathbf{H} are the magnetic field strengths, k the wave number, m the refractive index, then

$$(12) \quad k = 2\pi\lambda^{-1}$$

$$m^2 = \varepsilon - \frac{4\pi i\sigma}{\omega}$$

where λ is the wave-length, ω the angular frequency, ε a dielectric constant, σ the conductivity (for dielectric $\sigma = 0$). \mathbf{E} and \mathbf{H} in a homogeneous medium satisfy the general wave equation

$$\Delta \mathbf{A} + k^2 m^2 \mathbf{A} = 0$$

In polar three-dimensional coordinates φ , ϑ at a great distance r from the spherical source of scattering it holds for the intensity of the electromagnetic scattered wave:

$$(13) \quad \left\{ \begin{array}{l} \mathbf{E}_\vartheta = -\frac{i}{kr} \exp. [-ikr - i\omega t] \cos \varphi \mathbf{S}_2(\vartheta) \\ -\mathbf{E}_\varphi = -\frac{i}{kr} \exp. [i\omega t - ikr] \sin \varphi \mathbf{S}_1(\vartheta) \end{array} \right.$$

where

$$(14) \quad \mathbf{S}_1(\vartheta) = \sum_{n=1}^{\infty} \frac{2n+1}{n(n+1)} [a_n \tau_n(\cos \vartheta) + b_n \tau_n(\cos \vartheta)]$$

$$\mathbf{S}_2(\vartheta) = \sum_{n=1}^{\infty} \frac{2n+1}{n(n+1)} [b_n \tau_n(\cos \vartheta) + a_n \tau_n(\cos \vartheta)]$$

The values a_n ; b_n are given by

$$(15) \quad \left\{ \begin{array}{l} a_n = \frac{\psi'_n(y) \psi_n(x) - m \psi_n(y) \psi'(x)}{\psi'_n(y) \xi_n(x) - m \psi_n(y) \xi'(x)} \\ b_n = \frac{m \psi'_n(y) \psi(x) - \psi_n(y) \psi'(x)}{m \psi'_n(y) \xi_n(x) - \psi_n(y) \xi'_n(x)} \end{array} \right.$$

where

$$\begin{aligned}\psi_n(z) &= \sqrt{\frac{\pi z}{2}} J_{n+\frac{1}{2}}(z); & \xi(z) &= \sqrt{\frac{\pi z}{2}} H_{n+\frac{1}{2}}^{(2)}(z) \\ \pi_n(\cos \vartheta) &= \frac{1}{\sin \vartheta} P_n^{(1)}(\cos \vartheta); \\ \tau_n(\cos \vartheta) &= \frac{d}{d\vartheta} P_n^{(1)}(\cos \vartheta); & x = ka &= \frac{2\pi a}{\lambda}; & y &= mka\end{aligned}$$

$J_{n+\frac{1}{2}}(z)$ denotes a Bessel function of half order, $H_{n+\frac{1}{2}}^{(2)}(z)$ is the Hankel function of the second kind of half order, $P_n^{(1)}(\cos \vartheta)$ is the so-called conjugate Legendre polynomial. The dashed values of the functions ξ and ψ denote their derivatives. a = radius of particle (spherical), k = wave number = $\frac{2\pi}{\lambda}$, λ = wavelength, m = refractive index.

9. NUMERICAL RESULTS

Before going on to numerical calculations and evaluations of the different models of nebulae, let us recall the limiting assumptions since the accuracy of the results must be evaluated with regard to the assumptions on which the calculations were performed.

We assume particles of a nebula in the form of a sphere. We also assume that the scattered light has always the same frequency as the incident light. We thus eliminate any quantum transitions. A further limitation is the so-called scattering by independent particles. This means the assumption that all the individual particles are homogeneous but altogether they form an inhomogeneous medium, i. e. the individual particles are sharply bounded and separated from one another. The last physical assumption is so-called single scattering. Its significance consists in the direct proportionality of the intensity of the scattered light and the number of scattering particles, which is a consequence of the fact that each individual particle scatters only the light incident from the source and not the light already reflected (diffuse) from other particles. For greater details on the above assumptions we refer to the book by Van de Hulst [23]. The integrals in the relations with a view to the definition of the functions $\mathbf{S}_1(\vartheta)$ and $\mathbf{S}_2(\vartheta)$ can be calculated only by numerical integration. In all the cases of the different models we used Simpson's formulae for an approximate calculation of the limited integrals. The very complicated calculation of \mathbf{S}_1 and \mathbf{S}_2 as functions of ϑ is done on automatic computers and these functions are tabulated for different values of x and m , the definitions of which are given on page 9. The difficulty in calculating the scattering functions is clear also from the fact that tables hitherto have included a relatively small number of combinations of x and m . In Hulst's book, where there is a detailed list of tables of these functions, we find for example that up to 1957 the values of the scattering functions for m had not been calculated in the interval of 1.55 to 2. As will be shown below, these values of the refractive index would be particularly desirable for our purposes. The tabulated values of the scattering functions from [23] had to be used for a numerical calculation of the corresponding integrals.

The intensities at three distances from the centre of the nebula $0.25 r$, $0.5 r$ and $0.75 r$, where r is the unit distance from the centre to the edge of the nebula — were calculated for all the models of nebulae. It is obvious that at a distance $r = 1$ $I = 0$. In all the cases the calculations were made for the following wave-lengths of light: $\lambda_1 = 4100 \text{ \AA}$ and $\lambda_2 = 5500 \text{ \AA}$, and for three values of the refractive index $m = 1.33, 1.55, 2$. The unit distance r was chosen as $1/3$ of the observed radius of the nebula, i. e. $r = 12'$. In this way the correction for the dark mass in the surroundings is approximately made.

The correction with respect to absorption inside the nebula for a wave-length of 5500 \AA was made on the basis of the following: If the absorption in the nebula itself satisfies the relation

$$(16) \quad A \sim \lambda^{-1}$$

then we can assume that

$$\gamma = \frac{\lambda_2}{\lambda_2 - \lambda_1} = 3$$

In this case, since A is proportional to the optical depth, and the optical depth in our case is $\tau = kr$, we get $\lambda_2 = 1.5 \lambda_1$ i. e. the ratio of the radius of the nebula r_2 related to the wave-length $\lambda_2 = 5500$ to the real radius of the nebula r_1 is $r_2 = 0.7 r_1$.

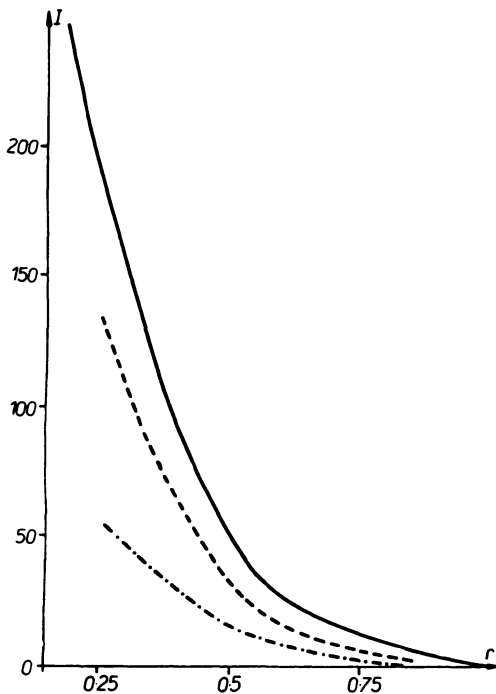


Fig. 2.

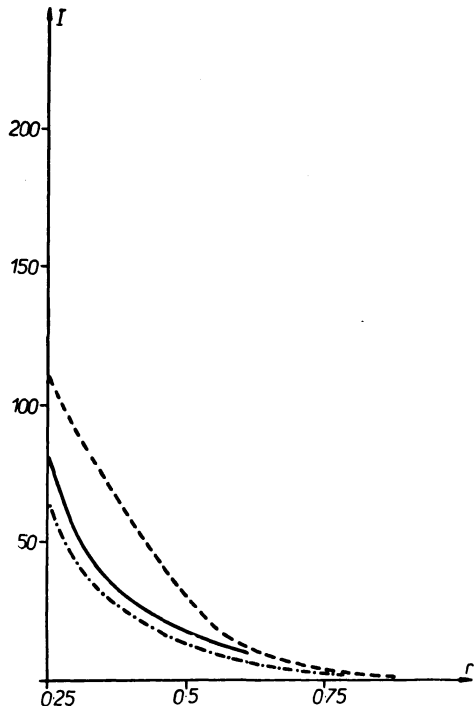


Fig. 3.

a) Spherical Nebula with Illuminating Star in Centre

This is the most important model for practical work. The calculation of the intensities is shown in graphs Nos. 2 (for λ 5500 Å) and 3 (for λ 4100 Å) in both case $a = 1950$ Å for the given wave-lengths.

If, now, we plot the dependence of the ratio $\frac{I_{\lambda_1}}{I_{\lambda_2}}$ on the distance from the centre of the nebula for different values of the refractive index, we obtain

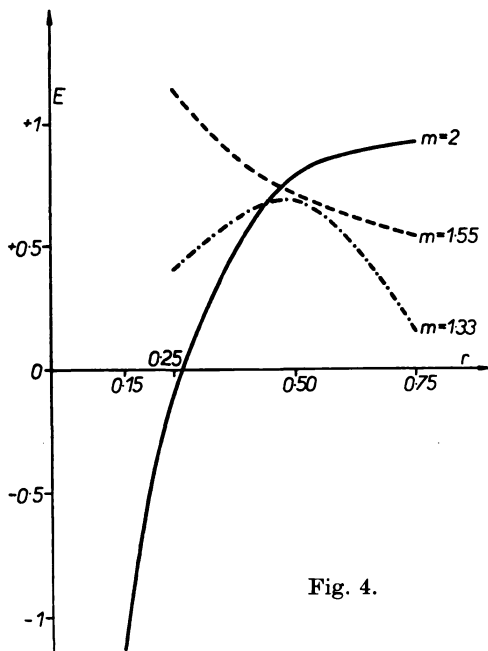


Fig. 4.

characteristic curves for the radius of the particle and for given refractive index. The dependences of the intensities on the distance in two wave-lengths of light can be obtained photographically or photoelectrically (photographical and visual). From these curves we calculate the ratio $\frac{I_{\lambda_1}}{I_{\lambda_2}}$ as a function of the distance.

We thus get by experimental means an analogous characteristic curve which we compare with the theoretical curves and therefore, at least in the first approximation, we can estimate the physical parameters of the particles of the nebula — dimension and refractive index. (fig. 4.)

Since

$$(18) \quad E = -2.5 \log \left[\frac{I_{\lambda_1}}{I_{\lambda_2}} \right]$$

we get simply from the ratio of the intensities the colour excess with respect to the illuminating star.

b) Nebula in Form of Spherical Layer, Where Illuminating Star is Further Along Direction of Line of Sight than Nebula

This model was calculated for $a = 3260$ Å, $\lambda = 5500$ Å and 4100 Å for $m = 1.33, 1.55, 2$. The dependence of the colour excess on the distance from the centre for the given values of the refractive index is given in graph No. 5a. The courses of the intensities for this model as well as for the other two are not plotted because the aim of this paper is to study colour excesses and their application to the physical parameters of particles. However, the results of calculating the intensities, on which they are based, are given for all models as a function of the distance and refractive index in Tab. VIII. Again it should be noted that the results in this table have only the significance of ratios. A comparison between graphs Nos. 4 and 5a is interesting. Despite the fact that these are two substantially different geometrical models, the curves of the colour excesses have a similar character, particularly for refractive indices of 1.33 and 1.55. However, for an index of refraction 2 the transition to negative values of the colour excess is much more intensive with the model of a nebula in the form of a spherical layer, where the illuminating star is further in the direc-

tion of the line of sight than the nebula. It can thus be said that the geometrical configuration substantially influences the "blueing" or "reddening" of reflection nebulae.

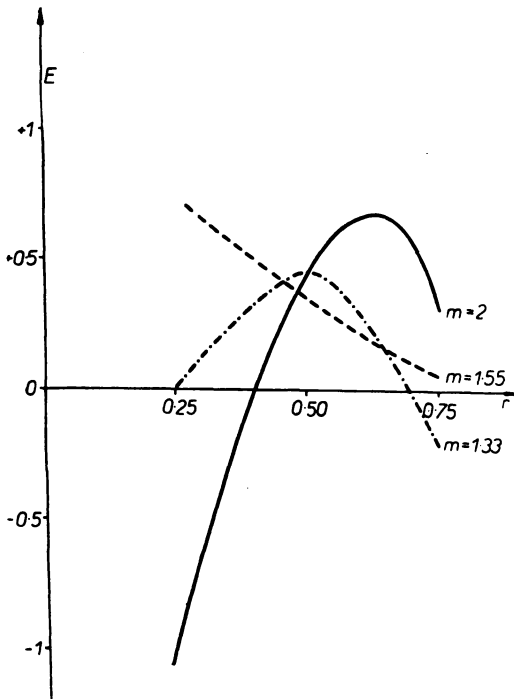


Fig. 5a.

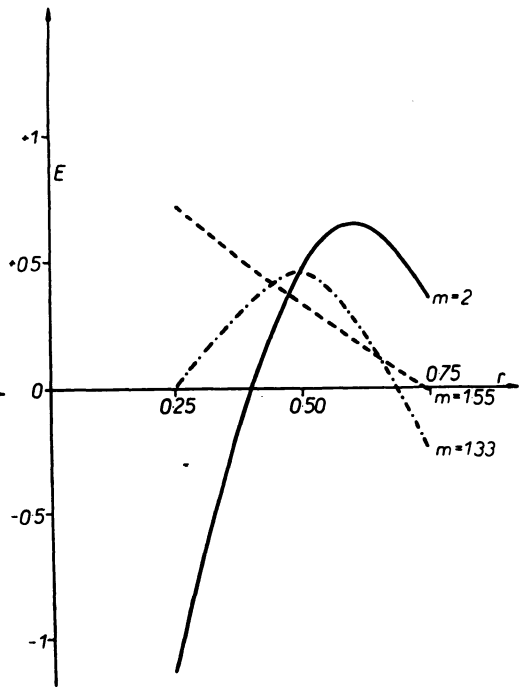


Fig. 5b.

Table VII. The colour difference E star-nebula NGC 7023

| | | | | E | |
|---------|------|--------------|-------------|--------------|------------------------|
| Keenan | 1936 | photogr. | $P_h - P_v$ | +0.23; -0.23 | 8 points |
| Collins | 1937 | photogr. | $P_h - P_v$ | -0.30 | 3 points |
| Martel | 1957 | photoelectr. | $P_h - P_v$ | -0.01; -0.41 | 6 points |
| Johnson | 1960 | photoelectr. | $B - V$ | -0.31 | 1 point 3'N |
| Vanysek | 1962 | photoelectr. | $B - V$ | +0.21; -0.50 | 3 tracings to $\pm 4'$ |
| Vanysek | 1963 | photoelectr. | $B - V (U)$ | -0.25 | 1 point 1'S |

c) Nebula in Form of Spherical Layer, Where Illuminating Star is Nearer in Direction of Line of Sight than Nebula

The calculation was performed for the same parameters as in the preceding case. Graph No. 6 again represents the courses of the colour excesses. A comparison of graphs Nos. 5a and 6 shows the absolutely different course of the curves of colour excesses. It is seen from Tab. VIII that the intensity of scattered light for both wave-length regions is up to a thousand times smaller in order in this model than in the corresponding cases of the preceding model. This

shows the important fact that this model, where the illuminating star is "in front", can be omitted when investigating this type. Even if we allowed that such formations occur in the universe they would be such weak objects that they would hardly be accessible to present-day observational and measuring techniques.

d) Nebula in Form of Annular Sphere

This model is given by the sum of the two preceding models. The dependences of the colour excesses (graph No. 5b) practically do not differ from those for model b). This is a logical consequence of the foregoing since the contributions

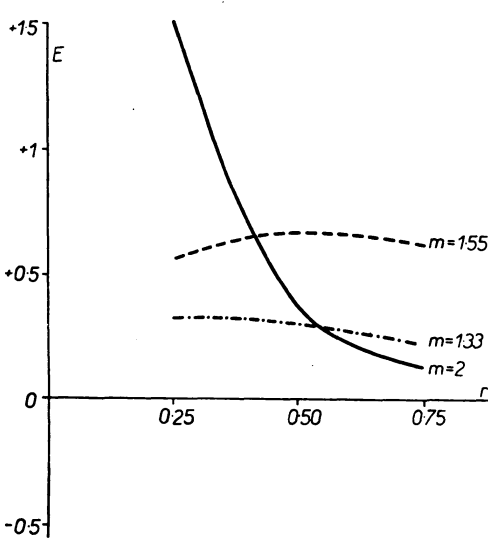


Fig. 6.

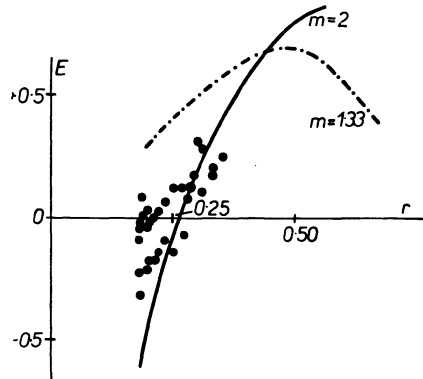


Fig. 7.

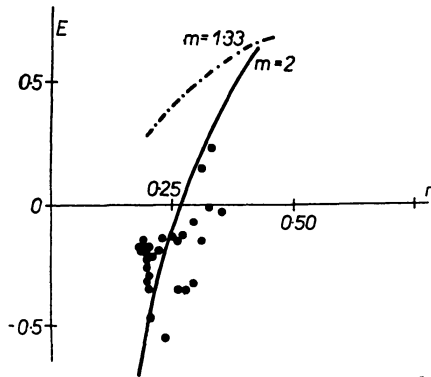


Fig. 8.

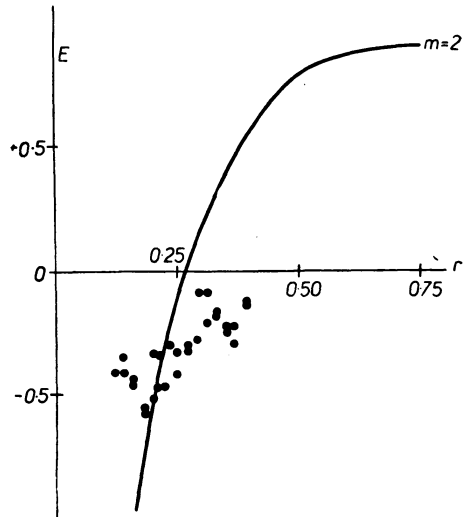


Fig. 9.

of the intensities in the model, where the illuminating star is “in front”, as has already been remarked, are negligible compared with the intensities scattered by the model with star “at the back”. Thus when studying the model in the form of an annular sphere the second term in brackets in relation (8a) can be neglected.

10. CONCLUSION

We naturally cannot expect that from the calculated and measured colour excesses we shall get an unambiguous and exact answer to the question of the composition and magnitude of particles of the nebula NGC 7023. The real conditions in this nebula are naturally far from satisfying all the limiting assumptions on which the calculation was performed. The experimental measurements also have their limitations. However, reliable measurements by either photoelectric or photographic means can be made relatively near to the centre (of illuminating star), i. e. in places where the nebula is still bright enough [8]. At greater distances from the centre the nebula is too weak while the measurements very near to the centre are affected by the disturbing influence of the illuminating star. The photoelectric measurement described above was performed approximately 0.10 to $0.25 r$ from the centre. The results are plotted in graphs Nos. 7, 8, 9. If the theoretical courses of the colour excess in the spherical nebula are plotted in these graphs a curve is obtained which agrees well in this interval with the course of the corresponding experimental values. This agreement is particularly clear in graphs Nos. 7 and 8. The experimental values, however, are displaced towards the centre while this displacement increases towards the centre.

This displacement, as we shall try to show below, can be explained by the fact that the nebula does not satisfy the assumption of a homogeneous sphere, i. e. the density decreases with distance from the centre. In order to prove that in the case of an inhomogeneous sphere the curves of the colour excesses are displaced towards the centre, let us consider the following: let there be a inhomogeneous sphere of given radius. For the sake of simplicity the inhomogeneity is represented as follows: inside the given sphere we imagine another sphere (homogeneous) of radius $r_a = \frac{1}{2} r$. Let the sphere of radius r_a have much higher density (than the region outside this sphere). Imagine that at a distance of e. g. $0.25 r$ we are measuring some intensities and their corresponding colour excess. These values therefore correspond to an inhomogeneous sphere of radius r . Neglecting now the region of small density, i. e. imagining away the dotted region, we find the same intensities at the same distance from the centre but we see that this distance corresponds now to the distance $0.5 r$, i. e. the distance corresponding to the homogeneous sphere. Simple calculation shows that when the theoretical and experimental curves coincide in the measured region the nebula must have a radius of $13'$. In actual fact this nebula has a radius of $18'$. We have thus obtained the quite natural result that the density in the nebula decreases with distance from the centre.

The disagreement between the theoretical and experimental curves in the region below 0.15 (graph No. 9) is also natural. In the region near to the star the density, on the basis of the above result, is so large that the assumption of so-called single scattering, mentioned at the beginning of section 9, is

far from being satisfied. This is in agreement with the optical depth for which the value of 1 was found on the basis of measuring the colour excess of the illuminating star. According to van den Hulst (23), however, for larger optical depths than 0.1 one must take into consideration the effect of multiple scattering. This problem is very difficult to solve exactly, however, and therefore we must avoid it by making a certain simplifying approximation as was done here. Although it is not possible mathematically to represent all the influences acting in a real nebula, the model of a spherical star cluster, where there is single scattering at least at greater distances from the nebula, can be regarded as sufficiently satisfactory. The results obtained justify us in the conclusion that the model containing particles of a dielectric nature, having refractive index 2 and dimension 0.33μ , is the most satisfactory. The interpretation concerning particles with refractive index 1 is somewhat questionable since here it was necessary that the nebula have much larger dimensions than follows from the apparent observable radius.

Another question is whether the solution would not be satisfied by models filled with semi-conducting heterogeneous particles, as is considered by Wickramasinghe for interstellar absorption. His calculations for carbon particles show a substantial growth in the albedo in the blue region of the visible spectrum of particles $0.03-0.05 \mu$ in dimension. As the author himself shows,

Table VIII.

| | 5500 Å | | | | 4100 Å | | |
|------------|---------|----------|----------|----------------------|---------|---------|---------|
| | 0.25 r | 0.5 r | 0.75 r | | 0.25 r | 0.5 r | 0.75 r |
| $m = 2$ | 0.199 | 0.0602 | 0.01797 | model 1 | 0.2133 | 0.0291 | 0.00761 |
| $m = 1.55$ | 0.621 | 0.0820 | 0.01998 | $a = 3260 \text{ Å}$ | 0.2174 | 0.0426 | 0.01221 |
| $m = 1.33$ | 0.451 | 0.0523 | 0.00743 | 0.33μ | 0.3111 | 0.0278 | 0.00639 |
| $m = 2$ | 0.1909 | 0.0487 | 0.01267 | model 1 | 0.08237 | 0.01666 | 0.00557 |
| $m = 1.55$ | 0.1337 | 0.03122 | 0.00617 | $a = 1950 \text{ Å}$ | 0.1076 | 0.02972 | 0.00387 |
| $m = 1.33$ | 0.05533 | 0.015883 | 0.003338 | 0.20μ | 0.06190 | 0.01222 | 0.00200 |
| $m = 2$ | 1.0972 | 1.2065 | 0.4879 | model 3 | 0.278 | 0.8618 | 0.4374 |
| $m = 1.55$ | 0.5767 | 1.2552 | 0.5253 | $a = 3260 \text{ Å}$ | 0.3427 | 0.6781 | 0.2957 |
| $m = 1.33$ | 0.08356 | 0.4141 | 0.1664 | 0.33μ | 0.06194 | 0.3124 | 0.1345 |
| $m = 2$ | 14.908 | 10.758 | 2.96 | model 2 | 42.4 | 6.960 | 2.202 |
| $m = 1.55$ | 84.773 | 15.618 | 3.643 | $a = 3260 \text{ Å}$ | 43.6 | 11.6213 | 3.684 |
| $m = 1.33$ | 72.781 | 10.105 | 1.274 | 0.33μ | 72.12 | 6.667 | 1.595 |
| $m = 2$ | 16.005 | 11.964 | 3.448 | model 4 | 42.678 | 7.822 | 2.639 |
| $m = 1.55$ | 85.350 | 16.873 | 4.168 | $a = 3260 \text{ Å}$ | 43.943 | 12.299 | 3.980 |
| $m = 1.33$ | 72.955 | 10.519 | 1.440 | 0.33μ | 72.182 | 6.979 | 1.729 |

A survey of the numerical results for the different models is given in Table VIII. This table gives a survey of the intensities for the different models as a function of the distance from the illuminating star, the refractive index and the wave-length. Of course, the intensities only have the significance of ratios; the two spherical models are mutually comparable but cannot be compared with the other models. However, the last three models can also be compared amongst themselves, i. e. the annular sphere and the spherical layers.

carbon particles could not explain the relatively high albedo that interstellar particles very probably have. He thus considers another model where the carbon particle is covered by a relatively thick layer of ice, and thus gets complicated ratios when calculating the scattering function — in his case, of course, he calculates only the ratio of the scattered and absorbed light, i. e. the albedo of the particle. It is seen that particles having a total dimension of 0.24 would best satisfy the dependence of the interstellar absorption on the wave-length, if, of course, the ratio of the radius of the carbon nucleus to the total dimension of the particle were 0.33μ . If we accepted our diameter for the interstellar particles, then the ratio of the diameter of the carbon nucleus, which seems most favourable around 0.08μ , to the total dimension of the particle would be 1 : 5. In such a case the albedo of the particles is very high — 0.8 and higher — and the refractive index, if its complex term is disregarded, approaches $m = 1.33$. A detailed theoretical study of light scattering in reflection nebulae for mixed types of particles will be the subject of further work.

Nevertheless it would be useful to make a similar investigation for dielectric particles with refractive index $m = 1.7$.

The question of multiple scattering near the centre of a nebula and the decrease in density of the nebula must also be taken into consideration in future.

The authors would like to thank P. Mayer for help in the observations and E. Vokalová for aid in the numerical treatment.

REFERENCES

- [1] SHAIN G., GAZE H., PIKELNER S. B.: Colloque International de Liège 1954, 441.
- [2] KEENAN P. C., ApJ 84, 600, 1936.
- [3] COLLINS O. C., ApJ 86, 529, 1937.
- [4] HENYCY L. G., GREENSTEIN J. L., ApJ 88, 580, 1938.
- [5] MARTEL T. M., AnAph Suppl. 7, 1958.
- [6] JOHNSON M. H., PASP 72, 10, 1960.
- [7] GEHLERS T., Bull. Lowell Obs., IV, 300, 1961.
- [8] GRYGAR J., Acta Univ. Carol., ser. Math., 1, 1959 (= Publ. Astr. Inst. Charles Univ., ser. II, No 25—26).
- [9] MENDOZA E. E., ApJ 128, 207, 1958.
- [10] HALL J. S., MIKESSELL A. H., Publ. USNO 17, pt. I, 1950.
- [11] JOHNSON H. L., Bull. Lowell Obs., IV, 43, 1958.
- [13] ROSINO L., ROMANO G., Contr. Asiago No. 127, 1962.
- [12] WATSON E. B., AJ 58, 48, 1953.
- [14] MAYER P., Acta Univ. Carol., ser. Math., No 1, 1964.
- [15] KHATCHIKIAN E., thesis, Erevan 1957.
- [16] PARSAMIAN E. S., Soobšč. Bjurakan 30, 57, 1962.
- [17] GREENSTEIN J. L., ALLER L. H., PASP 59, 139, 1957.
- [18] STEBBINS J., HUFFER C. M., WHITFORD A. E., ApJ 91, 20, 1940.
- [19] SCHALÉN C., Uppsala Ann. 1, No. 9, 1945.
- [20] VAN HOUTEN C. J., BAN 16, 509, 1961.
- [21] HOYLE F., WICKRAMASINGHE N. C., MN 124, 417, 1962.
- [22] WICKRAMASINGHE N. C., MN 126, 99, 1963.
- [23] VAN DE HULST H. C., Light scattering by small particles, London 1957.

SUMMARY

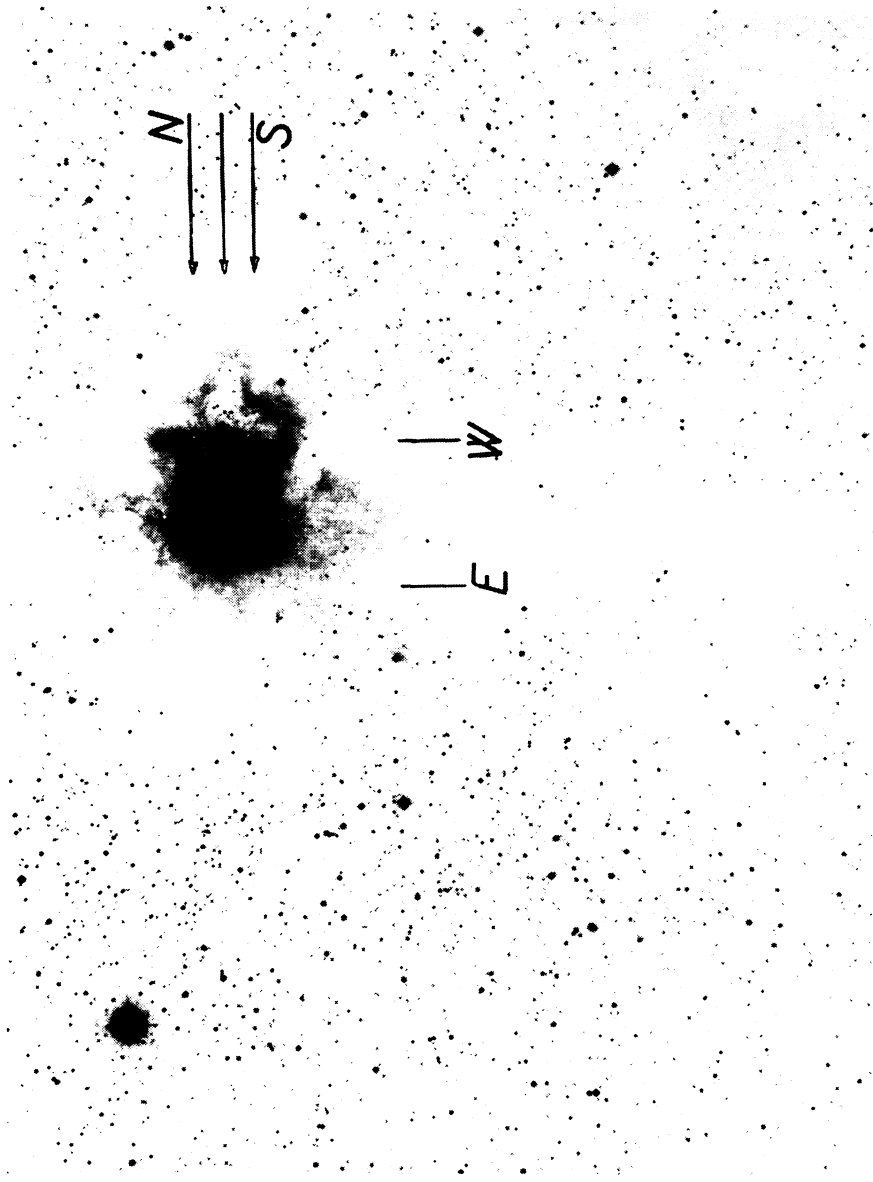
The first part of the paper gives the observational data of the reflexion nebula NGC 7023. The probable physical character of solid particles forming a nebula is studied on the basis of the selective light scattering of the illuminating star. Simple geometric models of the shape of a nebula with symmetrical location of the central star are calculated on the limiting assumption of single scattering. The models best suited to the observational course of the colour excess in the nebula are those which contain dielectric particles having refractive index $m = 2$ and 0.33μ in dimension. Ice particles, having refractive index $m = 1.33$, are somewhat less suitable and then only on certain assumptions — larger geometrical dimensions of nebula. It is assumed, of course, that the albedo of the particles is high, near to 1.

РЕЗЮМЕ

В настоящей первой части работы приводятся данные наблюдений отражательной туманности NGC 7023. На основании избирательного рассеяния света светящейся звезды изучается вероятный характер твердых частиц, образующих туманность. Рассчитывались простые геометрические модели формы туманности с симметрическим расположением центральной звезды при ограничивающем предположении однократного рассеяния. Моделями, наиболее удовлетворяющими ходу изменений избытка цвета в туманности являются модели содержащие диэлектрические частицы с показателем преломления $m = 2$ и размером $0,33 \mu$. Несколько менее и лишь при определенных условиях, а именно при более крупных геометрических размерах туманности, удовлетворяют ледяные частицы с показателем преломления $m = 1,33$. Однако предполагается, что альbedo частиц здесь имеет высокую величину и приближается к единице.

SOUHRN

V této první části studie jsou shrnuta pozorovací data reflexní mlhoviny NGC 7023. Na základě selektivního rozptylu světla osvětlující hvězdy je studován pravděpodobný fyzikální charakter pevných částic tvořících mlhovinu. Jsou počítány jednoduché geometrické modely tvaru mlhoviny se symetrickým umístěním centrální hvězdy za omezujícího předpokladu jednonásobného rozptylu. Modely, které by nejlépe vyhovovaly pozorovanému průběhu barevného excessu v mlhovině, jsou takové, které by obsahovaly dielektrické částice o indexu lomu $m = 2$ a rozměru $0,33 \mu$. Poněkud méně a jen za určitých předpokladů — většího geometrického rozměru mlhoviny — vyhovují částice ledové o indexu lomu $m = 1,33$. Předpokládá se ovšem, že albedo částic je vysoké, blízké 1.



On a reproduction of blue print of Palomar chart, the approximate directions of the photoelectric tracing on NGC 7023 are marked by arrows (north on the top). The E and W lines marked west and east limits of the measurements. Scale on reproduction is $28'' = 1 \text{ mm}$.